

# Novel Aspects Related to Nucleation and Growth of Solution Grown Polyethylene Single Crystals

Mingwen Tian,<sup>†</sup> Marcel Dosière,<sup>‡</sup> Stephan Hocquet,<sup>‡</sup> Piet J. Lemstra, and Joachim Loos\*

Department of Chemical Engineering and Chemistry and Dutch Polymer Institute, Eindhoven University of Technology, 5600 MB Eindhoven, The Netherlands

Received July 21, 2003; Revised Manuscript Received December 7, 2003

**ABSTRACT:** Within an intense research study concerning the theme “organization and reorganization of solution grown polyethylene single crystals”, the present part is focused on the nucleation and growth behavior of such crystals. Beside the well-known crystallization behavior, several novel features have been observed. Growth rates and the influence of the actual concentration on the growth rate have been analyzed using the technique of isochronous decoration. The most important results are that the growth rate decreases with decreasing concentration and that in our study the concentration coefficient  $\alpha$  is unit and independent of the crystallization temperature. Another feature is that the applied self-seeding temperature, above or below the dissolution temperature of PE in the solvent, determines the final organization of the crystals. Detailed analysis of the crystal fold surfaces using the *n*-alkane decoration technique has shown that the fold surfaces are regularly organized and have pronounced growth sectors when prepared at low seeding temperatures, but have no order of the fold surface when prepared using seeding temperatures above the dissolution temperature of PE.

## Introduction

Crystallization is the dominant (self-) organization process in polymers, the strongest driving force toward morphology formation. Understanding the crystallization behavior is a hot topic on the way to advanced materials for polymer devices and requires an integrated research approach. This includes the combination of fundamental polymer chemistry, physics, and engineering expertise on polymer crystallization and morphology formation, an understanding of the complex transitions of the materials investigated in time, and accurate theoretical descriptions of all these features.

During the last century several observations on, e.g., nucleation and growth rates of polymers crystallized from the melt or from solution have triggered the development of standard theories describing the crystallization of macromolecular materials and have formed the basis of our present understanding of crystallization. Looking in a modern textbook, one can find two somewhat different models explaining the crystallization of polymers: the “surface nucleation model”<sup>1</sup> and the “entropy barrier model”.<sup>2–4</sup> Although their physical origins are different, both models have successfully explained various experimental investigations related to the crystallization of polymers. However, both models use simple equilibrium physics approaches, which means that any stage from a noncrystalline state to the crystalline state is in equilibrium, but the metastable character of a common folded-chain crystal, e.g., reflected by the feature of lamellar thickening, is ignored.

Recent experimental results as well as computer simulation studies have shown that polymer crystallization is a rather complex phenomenon and that novel

and in particular nonequilibrium physics concepts are required to explain nucleation, growth, and organization of polymer crystals. Some of the recent observations are, e.g., the occurrence of density fluctuations already in the melt,<sup>5</sup> the observation of mosaic-blocks within lamellae,<sup>6,7</sup> and the thickening of lamellae from a mesomorphic phase.<sup>8</sup> Moreover, it seems that latest computer simulation studies are, at least partly, able to indicate organization processes during crystallization, which could explain the experimental observations mentioned.<sup>9–12</sup>

To contribute in this exciting research field and to understand features related to crystallization and melting of polymer crystals, in the present study the dominant theme is to follow the “life-cycle” of a solution grown polyethylene single crystal from its birth, the nucleation and growth, via aging including several reorganization processes to its death, the melting, and its possible rebirth, the recrystallization from the melt.

The surprising discovery that regular polymeric macromolecules (e.g., polyethylene) crystallize, not by forming fibers as might have been expected from filamentous molecules, but by forming thin folded-chain crystals with regular facets, with the chain direction almost perpendicular to the lamellar surface, has been one of the milestones in polymer science of the last century.<sup>13–16</sup> The observation of such folded-chain crystals formed both from the melt and from solution, and the investigation of their nucleation, growth, annealing, and melting has determined strongly the research activities in the field of polymer physics over more than four decades. Although progress has been and still is being made in our understanding of the morphology of crystalline polymers and, in particular the dynamic of organization and reorganization processes on the molecular level, the gaps in our knowledge are at present both wide and numerous.

The main analytical technique of choice is atomic force microscopy using various operation modes. Since the

\* Corresponding author: E-mail: j.loos@tue.nl.

<sup>†</sup> Permanent address: NT Instruments, Arnhemseweg 34d, 7331 BL Apeldoorn, The Netherlands.

<sup>‡</sup> Permanent address: Laboratoire de Physicochimie des Polymères, Université de Mons-Hainaut, Place du Parc, 20, 7000 Mons, Belgium.

**Table 1. Characteristics and Origin of the Linear Polyethylene Samples<sup>a</sup>**

$M_w$ (kmol/g)	$M_n$ (kmol/g)	$P$	supplier
4000	800	5.00	Hoechst AG
112	102	1.10	NIST

<sup>a</sup>  $M_w$  and  $M_n$  are the weight-average and number-average molecular weights, respectively;  $P$  is the polydispersity ( $\langle M_w \rangle / \langle M_n \rangle$ ).

**Table 2. Seeding Temperatures ( $T_S$ ) as a Function of Molecular Weights (from Refs 17–19)<sup>a</sup>**

$M_w$ (kmol/g)	$M_n$ (kmol/g)	$P$	solvent	$T_S$ (°C)
16	15	1.10	xylene	95.7
25	24	1.08	xylene	96.1
62	59	1.09	xylene	97.4
84	80	1.10	xylene	97.6
135			xylene	106.0
135			decalin	98.3
135			<i>p</i> -xylene	93.3
135			xylene	100.0
186	168	1.11	xylene	99.5
451	415	1.18	xylene	100.5

<sup>a</sup>  $M_w$  and  $M_n$  are the weight-average and number-average molecular weights, respectively;  $P$  is the polydispersity ( $\langle M_w \rangle / \langle M_n \rangle$ ).

invention of the scanning tunnel microscope (STM) by Binnig et al.<sup>17</sup> a whole family of scanning probe techniques has been developed. As one of these techniques, atomic force microscopy (AFM) is being widely applied for the characterization of polymer systems.<sup>18–24</sup>

In this part of the study, the focus is directed to understand the interaction between preparation conditions used, e.g., influence of molecular weight, concentration, and crystallization temperature used, the nucleation process, and the final organization of the formed single crystals. One specific research topic will be the investigation of the crystal formation dependent on the self-seeding temperature  $T_S$  used, which has had little attention in the past. It is not our intention to reproduce well-documented features; the main purpose of this study is to present and discuss novel experimental results.

## Experimental Section

**Preparation of Solution-Grown Polyethylene Single Crystals.** The materials used in the present studies are listed in Table 1. All samples are linear polyethylene.

The process of crystallization can be divided in two steps: the formation of stable nuclei, nucleation, and the growth of the crystals. For the preparation of polyethylene single crystals from solution within opportune times, the limiting factor is the nucleation step; from solution, it will be a homogeneous nucleation. To increase and to control the nucleation rate, the preparation technique of seeding or self-seeding has been developed.<sup>25</sup> By use of a smart pretreatment of the solution before initiating the crystallization process, the start conditions for crystal growth can be accurately controlled. In general, a solution is heated above the dissolution temperature of the polymer and then cooled to a rather low temperature where first crystallization starts (the solution becomes cloudy), heated again, but below the dissolution temperature ( $T_{Dis}$ , the solution becomes clear again), and subsequently cooled to the desired crystallization temperature.

It is important to know that temperatures commonly used for seeding depend on the molecular weight and concentration.<sup>25–27</sup> With increasing molecular weight and/or concentration the suitable seeding temperature increases. Some data for a fixed PE concentration of 0.1 wt % are listed in Table 2. However, in practice a whole temperature range of several degrees can be used for successful seeding of nuclei.

In the present study, polyethylene single crystals are prepared from dilute xylene solution by varying systematically

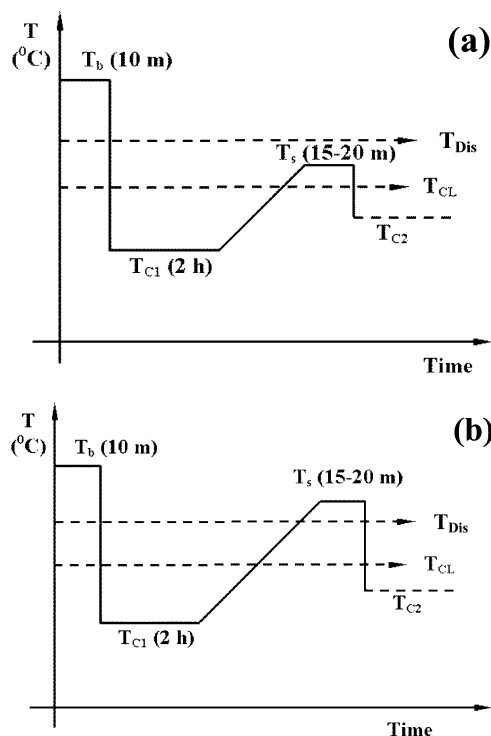


**Figure 1.** Typical temperature treatment to form single crystals: (a) common self-seeding procedure with  $T_{CL} < T_S < T_{Dis}$ ; (b) the so-called pseudo self-seeding procedure with  $T_{Dis} < T_S < T_b$ . Key  $T_b$ , boiling temperature of the solvent;  $T_S$ , self-seeding temperature;  $T_{CL}$ , “cloud-point” temperature where the cloud-like crystals disappear;  $T_{C1}$ , the temperature of first crystallization with the appearance of the cloud-like crystals;  $T_{C2}$ , isothermal crystallization temperature.  $T_{Dis}$  is the dissolution temperature.

$T_S$  for a given molecular weight, solvent and concentration. Dilute solutions with a concentration of 0.1–0.001 wt % for medium molecular weight PE and 0.001 wt % for ultrahigh molecular weight PE (UHMWPE) are applied throughout the whole study, if not indicated differently.

A typical preparation route is as follows: a PE/xylene solution is obtained by dissolving PE into the hot solvent at a temperature slightly below the boiling temperature ( $T_b$ ) of the solvent. The hot solution was transferred to an oil-bath, which had a temperature  $T_{C1}$ , and held for 2 h for the precrystallization (in principle, it is now a crystals in solvent suspension). Then it is heated to  $T_S$  with a heating rate of 10 °C/min and held for 15–20 min to form stabilized and uniform nuclei. Subsequently, the solution is transferred to another preheated oil bath having a temperature  $T_{C2}$ , which is the temperature for isothermal crystallization. A typically preparation sequence is described in Figure 1a. Moreover, sometimes a so-called “pseudo self-seeding” technique is applied for the preparation of crystals. In this case, the seeding temperature is above the dissolution temperature,  $T_S > T_{Dis}$  (Figure 1b).

For the measurements of the crystals growth, the crystals are removed from the solution at different crystallization times (minutes to days) by simply dipping freshly cleaved mica or small silicon wafer pieces in the solution followed by subsequent drying the samples in a vacuum oven at 40 °C for 24 h. The substrates used are preheated by immersing in a fresh solvent, which has a temperature similar to the crystallization temperature ( $T_{C2}$ ). This procedure is chosen to prevent the formation of nonisothermal crystallization of the remaining crystals in the solution due to the introduction of a cold substrate. Some of the samples are posttreated, e.g., annealed after deposition on the substrates.

**Isochronous Decoration Method.** The so-called isochronous decoration method is used to prepare PE single crystals.<sup>28–30</sup> Using this method the crystallization temperature is changed in a controlled way during the crystal growth. As seen in

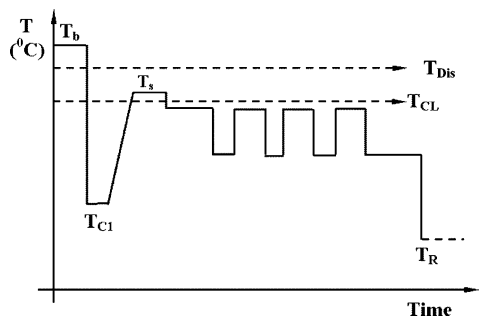


**Figure 2.** Temperature vs time profile of the isochronous decoration procedure. Key:  $T_s$ , self-seeding temperature;  $T_{CL}$ , "cloud-point" temperature where the cloud-like crystals disappear;  $T_{C1}$ , the temperature of first-crystallization with the appearance of the cloud-like crystals;  $T_R$ , room temperature.  $T_{Dis}$  is the dissolution temperature.

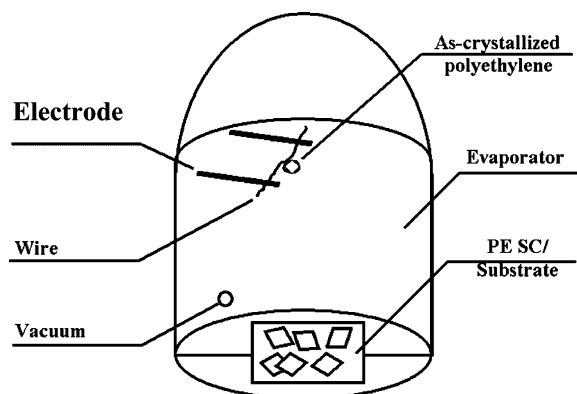


**Figure 3.** Sketch of the *n*-alkane decoration setup.

Figure 2 crystal bodies are prepared having alternating two different thicknesses, resulting from the two crystallization temperatures used. Changing the temperature during the crystallization process results in distinct thickness steps within the crystal body. A typical temperature transition time is  $\sim 10$  s. After crystallization, the single-crystal suspension is quenched to room temperature. Then, droplets of the solution are transferred onto the substrates as described above.

***n*-Alkane Decoration.** Some of the single crystals are decorated with *n*-alkanes following the route as described by refs 31 and 32. A detailed sketch of the setup can be found in Figure 3. For decoration purposes a linear polyethylene fraction is used having a weight-average molecular weight of  $\sim 55$  K and  $M_w/M_n \sim 4.5$ . A small piece of this material is placed on a  $\Omega$ -type wire in the evaporator. A vacuum below  $5 \times 10^{-5}$  mbar, a voltage of 20 V and a current of 30 A are used to uniformly decompose polyethylene. Moreover, a 15 cm distance between the sample and the wire in the vacuum evaporator is chosen to avoid possible surface melting of the PE single crystals. Using this setup the resulting *n*-alkanes condense on the surface of the single crystal and form rods by crystallization. The decoration is performed at room temperature. After decoration—and in the preferred case—the rods are aligned and form specific patterns, which may reflect the local organization of the fold surface of the crystal.

On the basis of electron diffraction studies<sup>31,32</sup> the alignment mechanism can be best demonstrated looking at Figure 4: the first condensed *n*-alkanes are considered as units searching for their most favorable organization and orientation on a fairly rough surface (at the chain diameter scale). Since ditches or furrows exist on the surface of the single crystals, which are formed by folds, loops, cilia, etc., the *n*-alkane chains align in a parallel way, rather than at an angle, to them. Subsequent accretion of the following *n*-alkane molecules results in the formation of oriented nuclei and, finally, of the rods. Because of its small size, the orientation of an *n*-alkane nucleus, and thus the orientation of the *n*-alkane rod, can be used to probe the local surface organization of the single crystals.

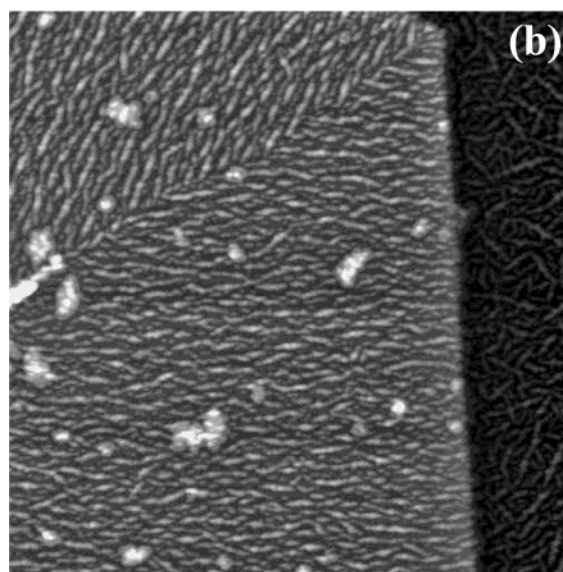
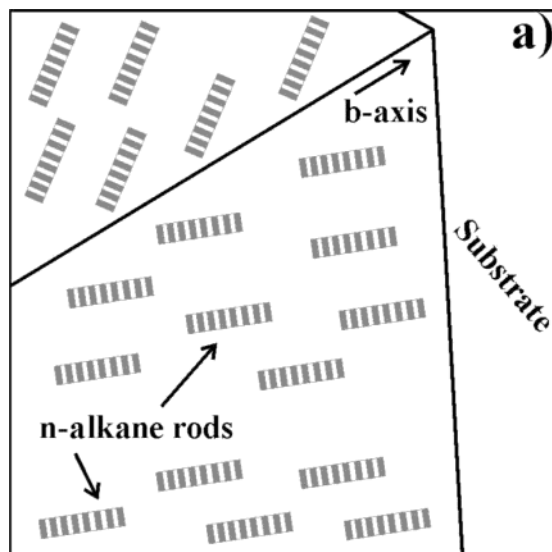


**Figure 4.** (a) Schematic representation of the substrate crystal and the orientation of the decorating *n*-alkane rods.<sup>24</sup> (b) High magnification height-contrast AFM image showing the orientations of *n*-alkane rods decorating two (110) sectors. Scanning size is  $3.0 \mu\text{m} \times 3.0 \mu\text{m}$ , and the height scale is 10 nm.

**Atomic Force Microscopy (AFM).** AFM investigations of the morphology evolution of PE single crystals are performed using a Smena P47H, NT-MDT Ltd., Moscow, Russia. The AFM is operated in noncontact mode in air using silicon cantilevers with spring constant  $k$  of 11–15 N/m, which are coated with a gold layer for higher laser beam reflectivity. Typical resonance frequencies are 210–230 kHz. The AFM has been calibrated using a 25 nm height standard grating produced by NT-MDT. Ltd., Moscow, Russia.

**Low Voltage Scanning Electron Microscopy (LVSEM).** Some morphology investigations of polyethylene solution-grown single crystals are performed using a Philips, at present Fei Co. (Eindhoven, The Netherlands) environmental scanning electron microscope XL30 ESEM-FEG, which is equipped with a field emission electron source, using low voltage mode (LVSEM) and a secondary electron detector. The detailed operation principle of LVSEM is described in ref 33.

After deposition of the polyethylene single crystals on mica or silicon wafer substrates the samples are investigated without any additional sample treatment using acceleration voltages between 700 V and 1 kV.

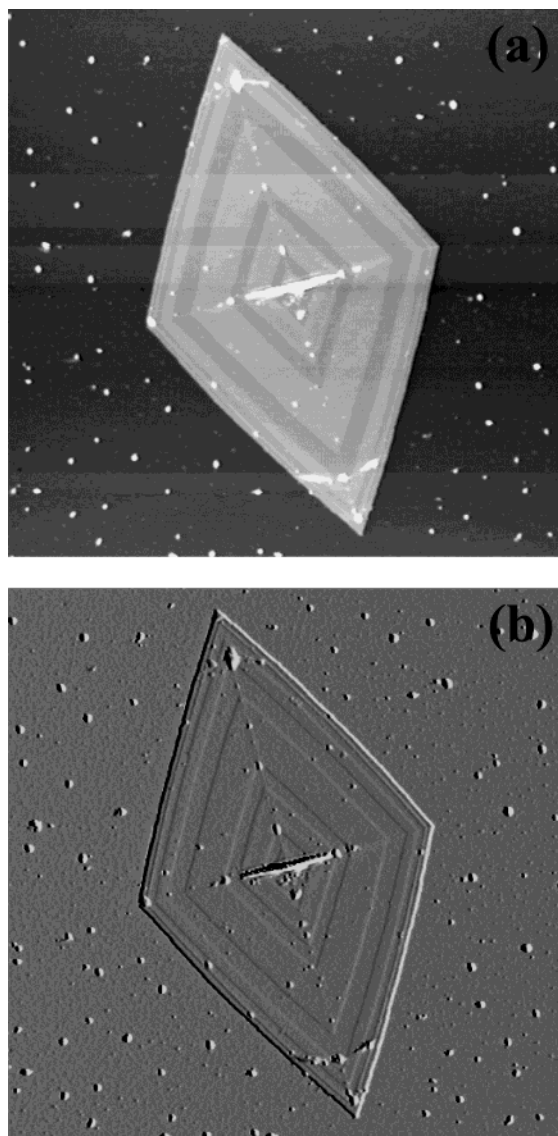


**Figure 5.** Single-crystal grown using the technique of isochronous decoration, the two different heights are visible, which correspond to the two different crystallization temperatures. (a) Height- and (b) amplitude-contrast images recorded by AFM in noncontact mode: scanning size is  $20\ \mu\text{m} \times 20\ \mu\text{m}$ ; height scale is 40 nm.

## Results and Discussion

**Growth Rate Determination Using the Isochronous Decoration Method.** For the exact determination of the growth rates of solution grown PE single crystals the technique of “isochronous decoration” has been used.<sup>28–30</sup> For this technique, a low concentrated solution of PE in xylene is prepared and nucleation is initiated using the self-seeding procedure. During the crystal growth the crystallization temperature is rapidly changed several times between two temperatures resulting in two different thicknesses within one individual lamella. A typical result is shown in Figure 5.

In this case, the initial PE concentration is 0.01 wt %, and the crystallization temperatures are 82 and 87 °C, respectively. It is obvious that the single crystal has a lozenge shape with rather smooth growth fronts, and the dominant central pleat indicates the self-seeding technique used. The pattern, which is a result of the changed crystallization temperature during the growth process, indicates two different thicknesses of the

**Table 3. Data Obtained from an Isochronous Decoration Experiment**

step (N)	$T_C$ (°C)	$T_I$ (min)	$L_N$ (nm)	$C_I$ ( $10^{-1}$ wt %)	$G_I$ (nm/min)	$L_D$ (nm)
1	87	16	944	0.1	59	14.8
2	82	1	532	0.0992	532	12.7
3	87	16	610	0.096	39	14.8
4	82	1	415	0.088	415	12.7
5	87	20	708	0.0817	35	14.8
6	82	2	602	0.0653	301	12.7
7	87	20	473	0.0504	24	14.8
8	82	4	610	0.0345	153	12.7
9	87	33	187	0.0149	5.7	14.8
10	82	1440	187	0.0070		12.7

<sup>a</sup> Key:  $T_C$ , crystallization temperature;  $T_I$ , crystallization time at temperature step  $I$ ;  $L_N$ , lateral distance from the center of the crystal to the growth fronts;  $C_I$ , the instant concentration;  $G_I$ , growth rate at  $I$  step; and  $L_D$ , crystal thickness including 2-fold surfaces.

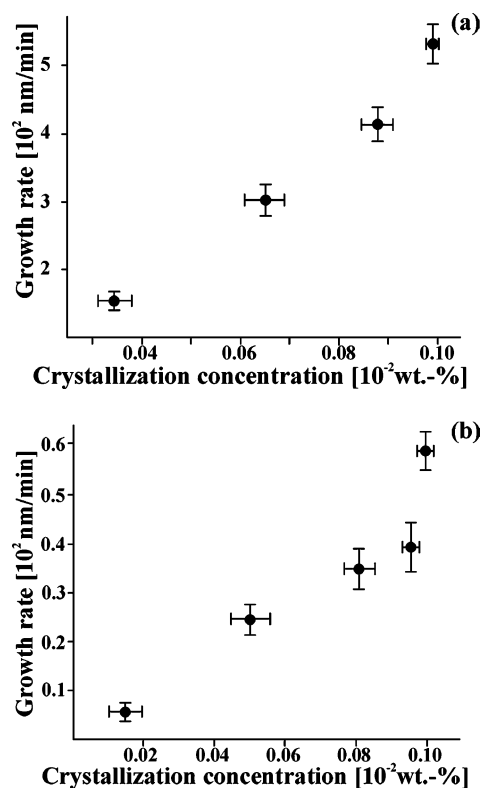


**Figure 6.** Growth rates as a function of the actual solution concentration for (a) 82 and (b) 87 °C.

lamella. Precise AFM measurements show that during the whole crystallization process both thicknesses are constant with  $\sim 12.7$  nm (for  $T_C = 82$  °C) and  $\sim 14.8$  nm (for  $T_C = 87$  °C), respectively, and thus are independent of the actual concentration in the solution.

Further, if one knows the crystallization time corresponding to one single growth step before changing again the temperature, accurate calculations of the actual PE concentration in the solution and the growth rate have been performed. The measured thickness and grow width data within the individual crystallization temperature steps and the calculated concentrations and growth rates are shown in Table 3.

From calculated growth rates as shown in Table 3 and plotted in Figure 6, it is evident that the growth rate decreases with lower polymer concentration in the solution. For the chosen crystallization temperatures an almost linear relation between growth rate and concen-

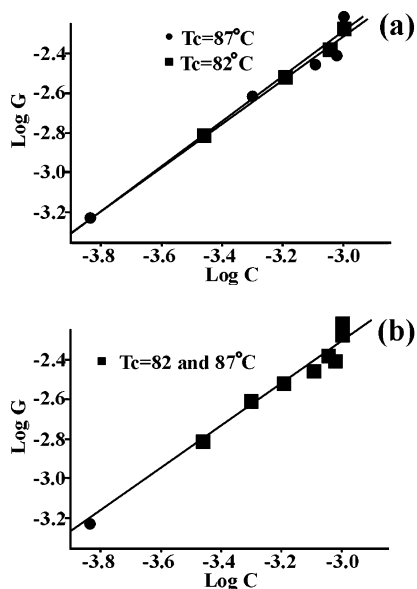


**Figure 7.** Double logarithmic plot of the growth rates vs concentration. (a) The lines indicate the linear fits for the crystallization temperatures of 82 and 87 °C, respectively, and (b) the linear fit of all data points together.

tration has been measured. In general, it is accepted that the growth rate decrease with increasing crystallization temperature for a given molecular weight and concentration of polymer in solution. This behavior could be confirmed within the present study. However, next to the parameters mentioned, the growth rate depends on the concentration. This relationship can be described by eq 1.

$$G \propto C^\alpha \quad (1)$$

Key:  $G$ , growth rate;  $C$ , concentration;  $\alpha$ , correction exponent.

In the literature the exponent  $\alpha$  has been calculated to be between 0.45 and 0.60, and to depend somewhat on crystallization temperature.<sup>34–36</sup> In the present study, the exponent  $\alpha$  could be calculated to be 1, and it shows no influence on the crystallization temperature (Figure 7). Such behavior may indicate that the growth of the lamellae is continuous even when increasing and decreasing the crystallization temperature several times during the experiment. However, this observation may be valid only for the experimental conditions used, and further experiments with varying crystallization temperatures, concentrations, and molecular weights have to be performed before the final conclusions can be drawn.

The observation that the exponent  $\alpha$  in eq 1 is independent of the crystallization temperature, for the experimental conditions used, may have some impact on our understanding of the nucleation process in the presence of a growth front having a thickness different from the thermodynamically stable thickness. In the case of a thicker substrate, such as in shish kebabs, it is in general accepted that for the secondary nucleation (the kebab) the surface free energy is reduced by the substrate (the shish). This yields to the formation of a transition zone, in which the folded chain crystal gradually decreases its thickness down to a thermodynamically stable value.<sup>37,38</sup> In contrast, the stable nucleus exceeds the thickness of the substrate if the crystallization temperature is increased (as in the

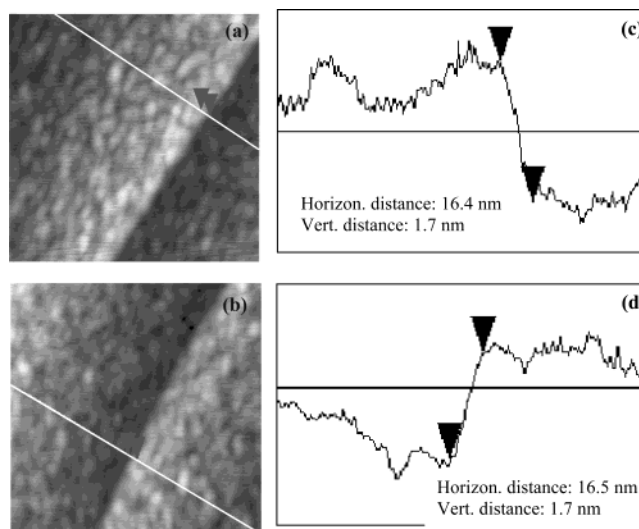


**Figure 8.** High magnification height-contrast images and their corresponding topography line scans on thickness steps formed at (a, c) decreasing and (b, d) increasing crystallization temperature; scan size is 400 nm  $\times$  400 nm. The topography line scans represent only a part of the lines drawn in the height images.

isochronous decoration experiments). Thus, in the latter case, there should be an induction time for nucleation, which certainly will slow the overall crystal growth rate, and should yield to a crystallization temperature-dependent exponent  $\alpha$ . However, this behavior could not be confirmed in the present study; the exponent  $\alpha$  is independent of the crystallization temperature. One conclusion from this observation is that the crystal growth is a continuous process and independent of the substrate size, and only depends on the access of molecules (which depends on the concentration).

To strengthen this observation, the crystal growth process is critically evaluated using the technique of isochronous decoration. Beside the clear evidence that, for the experimental setup used, less than 10 s are required for the stabilization of the crystallization temperature after a temperature change, morphological investigations of the thickness steps within the crystals have been performed. Figure 8 shows AFM height-contrast images of the thickness steps resulting from a decrease (Figure 8a, from 87 to 82 °C) or increase (Figure 8b, from 82 to 87 °C) of the crystallization temperature, and their corresponding topography line scans (Figure 8c,d).

Two apparent features can be observed from the images: a pattern spreading over the entire lamella, which might be caused by fold loops or by sedimented residues onto the lamella surface, and a rather sharp thickness step reflecting the crystallization temperature changed. In both cases the morphological appearance of the thickness step is identical having a height of  $\sim 1.8$  nm and a width of  $\sim 16.5$  nm, which might be in line with the statement of continuous nucleating and growing independent of the size of the substrate.

To further evaluate the correctness of the performed AFM measurements at the thickness steps for increasing and decreasing temperature jumps, a discussion of the influence of the AFM-tip size and shape on the height and especially on the lateral information accuracy has to be done. The tip has, in a two-dimensional representation, a hyperbolic shape with a contact area, which can be fitted as a circle. Because of this shape it

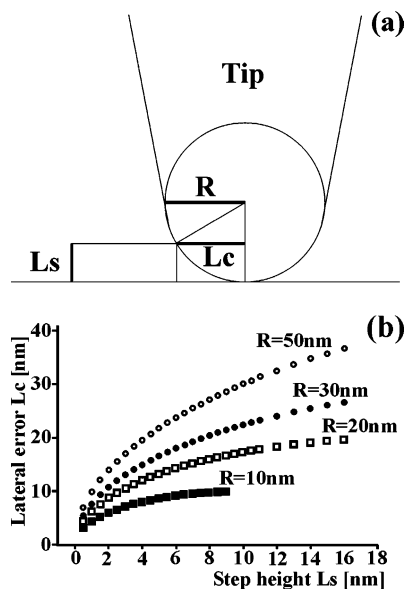


**Figure 9.** (a) Sketch of the tip-sample contact geometry,  $R$  is the tip radius,  $L_s$  the step height,  $L_c$  the lateral error. (b) Lateral uncertainty of AFM measurements depending on tip radius and step height.

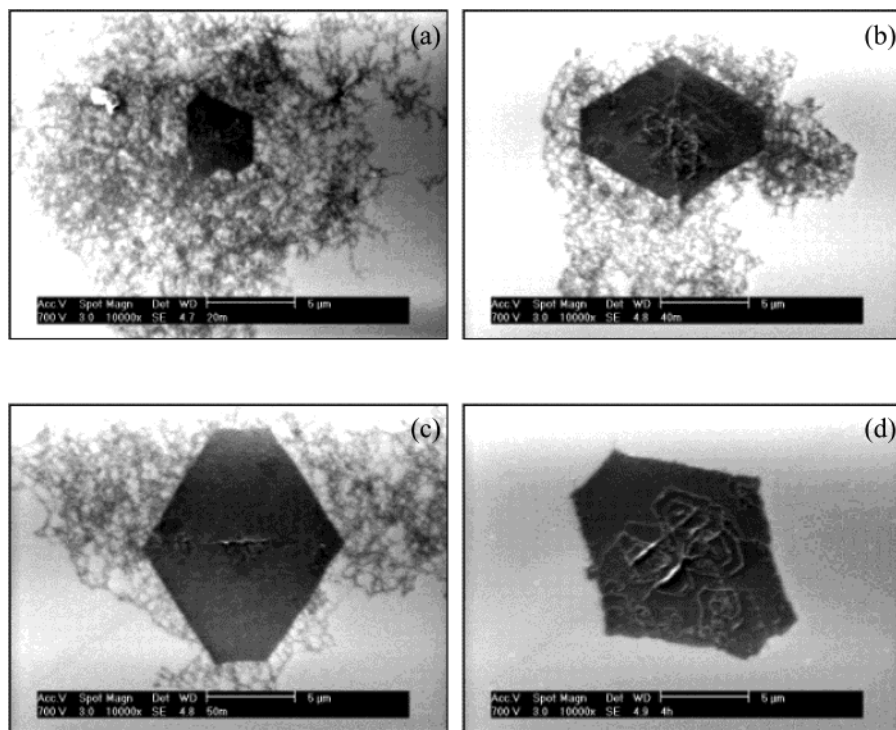
is possible that the tip interacts with the sample surface not only with, in the ideal case, a single atom located at the head of the tip, but infrequently also with its flanks, especially when the sample surface has some roughness or height steps.

Figure 9a represents a sketch of the tip geometry in contact with a rough sample surface. It is obvious that dependent on the tip radius and the height of the sample surface an error occurs in the lateral precision of the AFM measurement. Using simple geometric mathematics an approximation of this error can be done (Figure 9b). However, the calculations do not consider the effective tip-sample contact area, which depends on the

imaging conditions. For a height step of 2 nm, as in the case of the isochronous decoration experiment, even for a bad tip having a radius of 50 nm the exactness of lateral measurements is better than 15 nm, in the case of a standard tip having a radius of less than 10 nm a value of  $\sim 5$  nm for the imprecision of the lateral measurement can be achieved. Thus, the thickness gradient measured for decreasing as well as for increasing crystallization temperatures as shown in Figure 8 is a real feature. Of course, during the AFM measurements scan direction and scan speed as well as oscillation amplitude, etc. are systematically varied to prevent measurement artifacts. Thus, looking on the similar morphology of the thickness steps for increased or decreased crystallization temperature supports the observation that the exponent  $\alpha$  is independent of the crystallization temperature, and the growth process is continuous.

**Formation of Solution Grown Ultrahigh Molecular Weight Polyethylene Single Crystals.** The formation of solution-grown PE single crystals is followed. Crystals are fished from solution at several times, dried, and subsequently investigated using low voltage scanning electron microscopy and atomic force microscopy. An ultrahigh molecular weight PE is chosen for the experiments. Figure 10 shows a set of LVSEM images obtained after different crystallization time at a crystallization temperature of 85 °C. LVSEM is used mainly because it allows fast screening of a large sample area, which helps finding suitable crystals for imaging.<sup>33</sup> The images represent different crystals.

Using the self-seeding technique after a crystallization time of 20 min a single crystal is already formed, and its growth continues up to a crystallization time of approximately 1 h. Several morphological features can be seen in Figure 10: the truncated lozenge shape of the crystals and the central pleat. The crystals are surrounded and sometimes partly covered by residual



**Figure 10.** Set of LVSEM images of UHMWPE single crystals deposited on mica after crystallization in solution for (a) 20 min, (b) 40 min, (c) 50 min, and (d) 4 h.

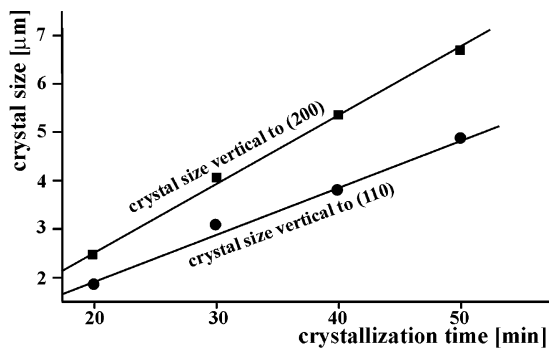


**Figure 11.** Plot of half the crystal size in  $\langle 200 \rangle$  and  $\langle 110 \rangle$  direction.

polymer material. It is evident that the amount of residual material decreases with increasing crystallization time, which indicates that the crystal growth process is almost finished after 50 min. In addition, from Figure 11 the growth rates of the crystals have been determined with 141 nm/min in  $\langle 200 \rangle$  direction and 97 nm/min in  $\langle 110 \rangle$  direction, respectively. In contrast to the isochronous decoration experiments described before, the influence of the reduced polymer concentration during crystallization cannot be measured.

As seen from Figure 10, the residual polymer material is only surrounding the growing crystals and cannot be found elsewhere onto the substrate, which might be an indication for some physical connection between the polymer chains still being in solution and the growth front of the lamellae. Of course, using a molecular weight of about 4000 kmol/g chain entanglements are an important issue and might explain the appearance of the residual molecules as dense network, even for the concentration of 0.001 wt % used. However, because they are located only nearby and in contact with the growing crystals some molecule parts might be already adsorbed at the growth front of the crystal, and it seems that the local polymer density at the growth front is enriched.

**Influence of the Self-Seeding Temperature Used on the Organization of the Crystals.** Systematic investigations are performed on the growth process of crystals treated according to the “pseudo” self-seeding technique using a seeding temperature of 105 °C for a PE having a molecular weight of 110 kmol/g dissolved at a concentration of 0.01 wt % in xylene and crystallized at 85 °C. Figure 12 shows typical LVSEM images of a sample immediately removed from the crystallization solution (Figure 12a), and a sample deposited on mica after crystallization for 6 h (Figure 12b). Because of the absence of seeds after short crystallization times

only small dendritelike structures can be found. However, there is clear evidence that already after few seconds some organization of the macromolecules in the solution is present, even for the high seeding temperature used. Another surprising feature is that already after crystallization for 6 h single crystals are present having pronounced lozenge shape and a size in  $\langle 010 \rangle$  direction on the order of 6 μm (Figure 12b). No central pleat or corrugation lines are visible, indicating that the crystal has been flat already in solution, instead of the hollow pyramidal shape of crystals self-seeded at lower temperatures. Calculations have demonstrated that applying the “pseudo” self-seeding the growth rate for the identical crystallization temperature (and identical concentration) is at least 1 order of magnitude lower than the growth rate for crystals prepared by the ordinary self-seeding procedure, in fact for the present case 3.9 vs 70.3 nm/min, respectively.

Figure 13a shows a typical solution grown crystal having truncated lozenge shape. The crystal is prepared from dilute xylene solution using a self-seeding temperature of 85 °C, which is  $T_S < T_{Dis}$ . Several morphological features can be discussed: the four  $\langle 110 \rangle$  and two  $\langle 200 \rangle$  sectors, the characteristic central pleat, and the pronounced corrugation lines around the pleat and within the  $\langle 200 \rangle$  sectors. In more detail, the central triangular pleat has an approximately triple-thickness compared with the lamella and is aligned along the crystallographic  $\langle 010 \rangle$  direction. Further, smooth lateral  $\{200\}$  and  $\{110\}$  growth faces and striations along the  $\langle 310 \rangle$  direction in the  $\langle 110 \rangle$  sectors or the  $\langle 200 \rangle$  direction in the  $\langle 200 \rangle$  sectors can be observed. These features indicate that the crystal has had a hollow pyramidal shape in the solution and has been collapsed during the process of sedimentation on a substrate.<sup>39,40</sup>

In contrast, Figure 13b shows a crystal grown via the preparation route of setting  $T_S > T_{Dis}$  ( $T_S = 105$  °C). This crystal has a lozenge shape with a smooth folding surface and rough lateral growth planes. Since there is neither a characteristic central pleat along the crystallographic  $\langle 010 \rangle$  direction nor pronounced corrugation lines, it is expected that the original crystals has been flat already in the solution before sedimentation.

On the basis of the observation that depending, whether the self-seeding ( $T_S < T_{Dis}$ ) or pseudo self-seeding ( $T_S > T_{Dis}$ ) preparation technique is applied, the appearance of the single crystals is different further experiments are performed. Both “types” of crystals are treated using the *n*-alkane decoration technique.<sup>31,32</sup> Figure 14 shows two AFM images in height contrast. In the case of following the standard self-seeding procedure alignment of the *n*-alkane rods parallel to the

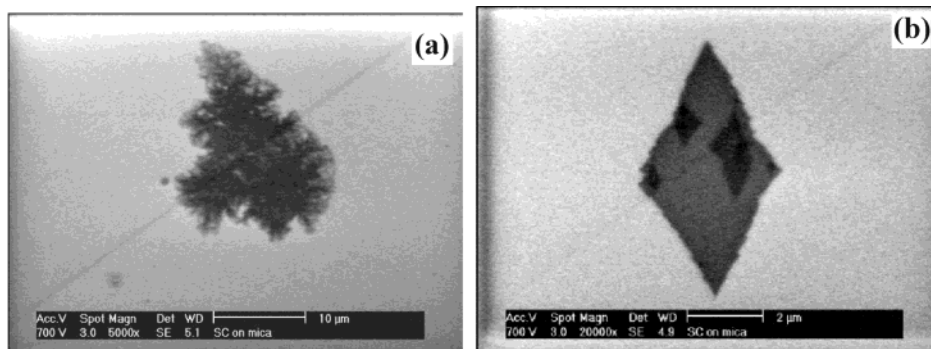


**Figure 12.** LVSEM images of PE single crystals deposited on mica after growing in solution at 85 °C for (a) few seconds and (b) 6 h. Seeding temperature  $T_S$  is 105 °C.

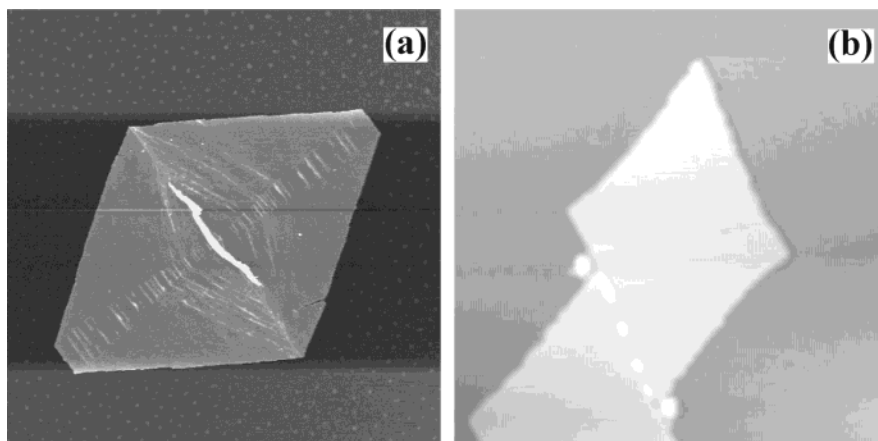


**Figure 13.** Height contrast images recorded on (a) a truncated lozenge PE single crystal prepared from solution by the common self-seeding technique, scanning size is  $10\ \mu\text{m} \times 10\ \mu\text{m}$ , height scale is 100 nm, and (b) a lozenge shaped crystal grown using the pseudo-self-seeding procedure with  $T_S = 105\ ^\circ\text{C}$ . Scan size is  $5\ \mu\text{m} \times 5\ \mu\text{m}$ ; height scale is 50 nm.

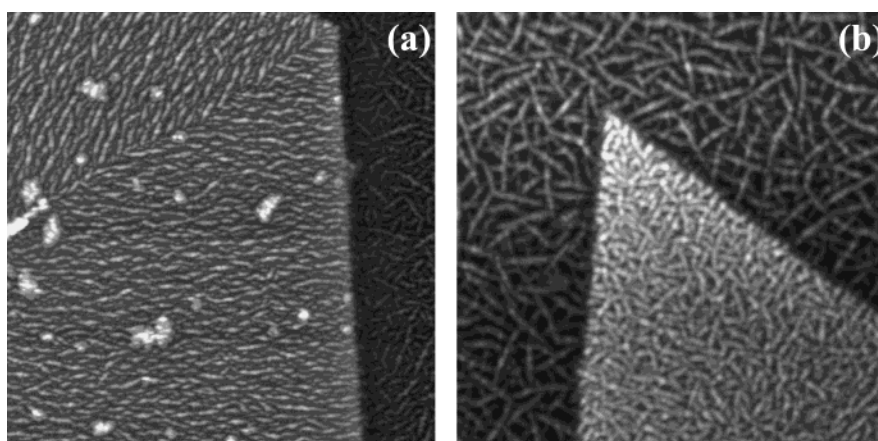


**Figure 14.** Height contrast AFM images of *n*-alkane decorated single crystals: (a)  $T_S < T_{\text{Dis}}$  (same as Figure 4b) and (b)  $T_S > T_{\text{Dis}}$ . Scan size is (a)  $3\ \mu\text{m} \times 3\ \mu\text{m}$  and (b)  $2\ \mu\text{m} \times 2\ \mu\text{m}$ , respectively, and the height scale is 10 nm.

$\langle 110 \rangle$  direction with a clear border between two sectors can be seen. The right side of the image represents *n*-alkane rods laying on the mica substrate. In contrast, using the pseudo-self-seeding technique, which means that the seeds are completely destroyed before starting the isothermal crystallization, no pronounced surface organization can be detected. A possible explanation might be that in the latter case the organization of the crystal is much disordered. More details on the organization of the crystals will be discussed in other parts of our study.

## Conclusions

In the present part of the study concerning the organization and reorganization of solution grown polyethylene single crystals, the nucleation and growth process of such crystals has been analyzed. The influence of several preparation parameters, such as molecular weight, concentration, crystallization temperature and seeding temperature, has been systematically investigated. Main experimental observations are as follows.

- An apparent relation between actual polymer concentration during one crystallization experiment and the crystal growth rate could be established. It should be noted that Doisère et al. have already discussed a similar relationship between actual polymer concentration and growth rate.<sup>29</sup> However, at that time no quantitative calculation of the concentration could be

performed, because of the lack in local quantitative thickness data.

- For the experimental conditions used the concentration coefficient  $\alpha$  could be calculated to be unit and independent of the crystallization temperature.

- Within the experimental accuracy the secondary nucleation at the growth front of a crystal is independent of the length of the substrate (as seen from the isochronous decoration experiments).

- To the best of our knowledge it is the first time that individual solution-grown ultrahigh molecular weight polyethylene single crystals could be prepared.

- Attachment of individual molecules and increase of local polymer density at the crystal growth front could be observed. Even for dilute concentrations chain entanglements are present near to the growth front.

- The (“pseudo”) self-seeding temperature determines shape and organization of the single crystals. For low temperatures ( $T_S < T_{\text{Dis}}$ ) initial hollow pyramidal crystals with clear sectorization are grown in solution, at high temperatures ( $T_S > T_{\text{Dis}}$ ) the crystals are already flat in the solution and, at least, their surfaces are disordered (seen from *n*-alkane decoration experiments).

- An unexpected high growth rate for crystals prepared by the “pseudo” self-seeding technique ( $T_S > T_{\text{Dis}}$ ) has been found: crystals are already formed after minutes to hours, instead of days to weeks (as stated in the literature).

•Atomic force microscopy and low voltage scanning electron microscopy are accurate techniques for morphological investigations of polymer single crystals. In particular, AFM can be used for quantitative lateral size and height measurements.

**Acknowledgment.** We would like to acknowledge the Dutch Polymer Institute (DPI) for support of the presented study. The authors also thank Jürgen Petermann, Ingo Lieberwirth, Bernard Lotz, Jamie Hobbs, Jens-Uwe Sommer, and Sanjay Rastogi for their indefatigable readiness for discussions. Also the support of the people from NT-MDT should be mentioned.

## References and Notes

- (1) Lauritzen, J. I.; Hoffman, J. D. *J. Res. Natl. Bur. Stand.* **1960**, *64*, 73.
- (2) Sadler, D. M.; Gilmer, G. H. *Phys. Rev. Lett.* **1986**, *56*, 2708.
- (3) Sadler, D. M. *Nature (London)* **1987**, *326*, 174.
- (4) Sadler, D. M.; Gilmer, G. H. *Phys. Rev.* **1988**, *B38*, 5684.
- (5) Olmsted, P. D.; Poon, W. C. K.; McLeish, T. C. B.; Terrill, N. J.; Ryan, A. J. *Phys. Rev. Lett.* **1998**, *81*, 373.
- (6) Hugel, T.; Strobl, G.; Thomann, R. *Acta Polym.* **1999**, *50*, 214.
- (7) Loos, J.; Thüne, P. C.; Lemstra, P. J.; Niemantsverdriet, J. W. *Macromolecules* **1999**, *32*, 8910.
- (8) Rastogi, S.; Hikosaka, M.; Kawabata, H.; Keller, A. *Macromolecules* **1991**, *24*, 6384.
- (9) Doye, J. P. K.; Frenkel, D. *Phys. Rev. Lett.* **1998**, *7*, 2160.
- (10) Doye, J. P. K.; Frenkel, D. *J. Chem. Phys.* **1999**, *110*, 2692.
- (11) Doye, J. P. K.; Frenkel, D. *J. Chem. Phys.* **1999**, *110*, 7073.
- (12) Muthukumar, M.; Welch, P. *Polymer* **2000**, *41*, 8833.
- (13) Stokes, K. H. *J. Am. Chem. Soc.* **1938**, *60*, 1753.
- (14) Keller, A. *Philos. Mag.* **1957**, *2*, 1171.
- (15) Till, P. H. *J. Polym. Sci.* **1957**, *24*, 301.
- (16) Fischer, E. W. *Z. Naturforsch.* **1957**, *A12*, 753.
- (17) Binning, G.; Rohrer, H.; Gerber, C.; Weibel, E. *Appl. Phys. Lett.* **1982**, *40*, 178.
- (18) Nakagawa, Y. *Denshi Kenbikyo* **1997**, *32*, 5.
- (19) Schönherr, H.; Snetivy, D.; Vancso, G. *J. Polym. Bull. (Berlin)* **1993**, *30*, 57.
- (20) Zhou, H.; Wilkes, G. *J. Polymer* **1997**, *38*, 5735.
- (21) Magonov, S. N.; Whangbo, M. H. *Surface Analysis with STM and AFM*; VCH: Weinheim, Germany, 1996.
- (22) Zhou, W.; Cheng, S. Z. D.; Putthanarat, S.; Eby, R. E.; Reneker, D. H.; Lotz, B.; Magonov, S.; Hsieh, E. T.; Geerts, R. G.; Palackal, S. J.; Hawley, G. R.; Welch, M. B. *Macromolecules* **2000**, *33*, 6861.
- (23) Hobbs, J. K.; Miles, M. J. *Macromolecules* **2001**, *34*, 353.
- (24) Hobbs, J. K.; Miles, M. J. *Macromolecules* **2001**, *34*, 5508.
- (25) Blundell, D. J.; Keller, A.; Kovacs, A. J. *Polym. Lett.* **1966**, *4*, 487.
- (26) Holland, V. F. *J. Appl. Phys.* **1964**, *35*, 59.
- (27) Coran, A. Y.; Anagnostopoulos, C. E. *J. Polym. Sci.* **1962**, *57*, 13.
- (28) Point, J. J.; Colet, M. Ch.; Dosière, M. *J. Polym. Sci., Polym. Phys.* **1986**, *24*, 357.
- (29) Dosière, M.; Colet, M. Ch.; Point, J. J. *J. Polym. Sci., Polym. Phys.* **1986**, *24*, 345.
- (30) Dosière, M.; Colet, M. C.; Point, J. J. *Morphol. Polym., Proc., Europhys. Conf. Macromol. Phys. 17th* **1986**, 171–178.
- (31) Wittmann, J. C.; Lotz, B. *Makromol. Chem. Rapid. Commun.* **1982**, *3*, 733.
- (32) Wittmann, J. C.; Lotz, B. *J. Polym. Sci., Polym. Phys.* **1985**, *23*, 205.
- (33) Loos, J.; Tian, M. *e-Polym.* **2002**, *36*, www.e-Polym.org.
- (34) Cooper, M.; Manley, R. St. J. *Macromolecules* **1975**, *8*, 219.
- (35) Keller, A.; Pedemonte, E. *J. Cryst. Growth.* **1973**, *18*, 11.
- (36) Sanchez, I. C.; Dimarzio, E. A. *Macromolecules* **1971**, *4*, 677.
- (37) Loos, J.; Katzenberg, F.; Peterman, J. *J. Mater. Sci.* **1997**, *12*, 1551.
- (38) Martinez-Salazar, J.; Garcia Ramos, J. V.; Petermann, J. *Int. J. Polym. Mater.* **1993**, *21*, 111.
- (39) Bassett, D. C.; Keller, A. *Philos. Mag.* **1962**, *7*, 1553.
- (40) Bassett, D. C.; Frank, F. C.; Keller, A. *Philos. Mag.* **1963**, *8*, 1753.

MA035042X